

Relativistic Anyon Beam: Construction and Properties

Joydeep Majhi,¹ Subir Ghosh,¹ and Santanu K. Maiti¹

¹*Physics and Applied Mathematics Unit, Indian Statistical Institute,
203 Barrackpore Trunk Road, Kolkata-700 108, India*

Motivated by recent interest in photon and electron vortex beams, we propose the construction of a relativistic anyon beam. Following Jackiw and Nair [Phys. Rev. D **43**, 1933 (1991)] we derive explicit form of relativistic plane wave solution of a single anyon. Subsequently we construct the planar anyon beam by superposing these solutions. Explicit expressions for the conserved anyon current are derived. Finally, we provide expressions for the anyon beam current using the superposed waves and discuss its properties. We also comment on the possibility of laboratory construction of anyon beam.

We propose construction of a relativistic beam of anyons in a plane. Anyons are planar excitations with arbitrary spin and statistics. The procedure is similar to 3D optical (spin 1) and electron (spin 1/2) vortex beam.

Vortex beams, of recent interest, carrying intrinsic orbital angular momentum are non-diffracting wave packets in motion. In 3D, vortex beams for photons and electrons were proposed by Durnin *et al.* [1] and by Bliokh *et al.* [2] respectively (see [3]). Properties and experimental signatures of twisted optical and electron vortex beam were studied respectively in [4] (for spinless electron [2]) and [5] (spinor electron [2]). Wave packets were constructed out of free plane wave, orbital angular momentum solutions having vorticity. In 3D, non-trivial Lie algebra of rotation generators along with finite dimensional representations of angular momentum eigenstates restricts the angular momentum to quantize in units of $\hbar/2$. Absence of such an algebra in 2D allows excitations (anyons [6, 7]) with arbitrary spin and statistics with infinite dimensional representations. Here, we construct directed transversely localized anyon wave packet or wave beam in 2D.

Geometry imposes a qualitative difference between monoenergetic wave packet and wave beam both in 3D and 2D. In 3D the wave packet is described by three discrete quantum numbers as it is localized in three directions whereas ideally an energy dispersionless wave packet where wave components having identical momentum along the direction of propagation will be completely delocalized along that direction and will constitute a beam [1, 2]. But, in 2D a monoenergetic wave beam will necessary have dispersion in momentum along propagation direction and hence cannot be completely delocalized. The delocalization along propagation direction will be more for narrower angle of superposition.

Apart from earlier interest [6], graphene also involves anyons [9]. Non-Abelian anyons [10] are touted as theoretical building blocks for topological fault-tolerant quantum computers [11]. An exact chiral spin liquid with non-Abelian anyons has been reported [12]. The direct observational status of anyons has shown promising development [13].

The *minimal* field theoretic and relativistic model of a single anyon was constructed by Jackiw and Nair (JN) [14]. JN anyon is the most suitable one that serves our purpose since, being first order in spacetime derivatives, it closely resembles the Dirac equation used by [2]. A major difference is that unitary representation for arbitrary spin JN anyon requires an *infinite* component wave function [15], (to maintain covariance), along with subsidiary constraints that restrict the number of independent components to a single one [14].

We propose: (i) an explicit form of the single anyon solution of the JN anyon equation [14] (which is a new result), (ii) anyon conserved current (again a new result), (iii) anyon wave packet in 2D, (iv) anyon wave packet in the conserved current that constitutes the anyon beam, (v) anyon charge and current densities for the anyon beam numerically since closed analytic expressions could not be obtained, (vi) possible laboratory setup for observing anyon beams, and (vii) finally, future prospects. The new results (i, ii) lead us to our principal outputs (iii, iv) and hopefully (v).

(i) **Jackiw-Nair anyon equation and its solution:** We start with a familiar system, free spin one particle in $2 + 1$ -dimensions [14]. The dynamical equation in co-ordinate and momentum space ($i\partial_a = p_a$) is given by

$$\partial_a \epsilon^{abc} F_c \pm m F^b = 0; \quad (p \cdot j)_b^a F^b + m s F^a = 0. \quad (1)$$

The solution of the three-vector F^a , $a = 0, 1, 2$ (we use Minkowski metric $\eta_{\mu\nu} = \text{diag}(1, -1, -1)$) is given by

$$F^a(p) = \frac{1}{\sqrt{2}} \left[\begin{array}{c} 0 \\ 1 \\ i \end{array} \right] + \frac{p^x + ip^y}{m(E+m)} \left[\begin{array}{c} E+m \\ p^x \\ p^y \end{array} \right] \sqrt{\frac{m}{E}}. \quad (2)$$

The same F^a can also be expressed as a Lorentz boosted form

$$F^a(p) = B_b^a(p)N_c^b F_0^c(p), \quad N_c^b = \frac{1}{\sqrt{2}} \begin{bmatrix} \sqrt{2} & 0 & 0 \\ 0 & 1 & i \\ 0 & -i & i \end{bmatrix} \quad (3)$$

where the boost is expressed by the generators j^a

$$\begin{aligned} B(p) &= e^{i\Omega_a(p)j^a}; [B(p)]_b^a = [B^{-1}(p)]_b^a \\ &= \delta_b^a - \frac{(p^a + \eta^a m)(p_b + \eta_b m)}{m(p \cdot \eta + m)} + \frac{2p^a \eta_b}{m} \end{aligned} \quad (4)$$

with $\eta_a = (1, 0, 0)$. It is straightforward to check that F^a describes a spin one particle ($s = 1$) of mass m .

This construction has been extended in an elegant way to the JN anyon equation [14] to describe an anyon of arbitrary spin $s = 1 - \lambda$, whose dynamics in momentum space is given by,

$$P \cdot (K + j)_{an \ a'n'} f_n^{a'} + m s f_{an} = 0, \quad (D_a f^a)_n = 0, \quad (5)$$

($D_{nn'}^a = \epsilon_{bc}^a P^b K_{nn'}^c$) where the second equation is the subsidiary (constraint) relation. For $\lambda = 0$ the anyon reduces to the spin one model discussed earlier [14]. The actions of j^a, K^a are given by

$$\begin{aligned} P \cdot K_{an \ a'n'} &= P \cdot K_{nn'} \delta_{aa'}, \quad P \cdot j_{an \ a'n'} = P \cdot j_{aa'} \delta_{nn'}; \\ K_{nn'}^a &= \langle \lambda, n \mid K^a \mid \lambda, n' \rangle, \quad (j^a)_{a'a''} = i \epsilon_{a'a''}^a \end{aligned}$$

Generalizing the spin-1 case (3), the free anyon solution is formally given by [14]

$$f_n^{a(\pm)}(p) = B_{n0}(p) B_b^a(p) N_c^b f^{c(\pm)}(p), \quad (6)$$

where $B_{nn'}(p), B_b^a(p)$ are the spin λ and spin 1 representations of the boost transformation respectively and N_c^b is the same numerical matrix as in (3).

Exploiting coherent state formalism for $SU(1, 1)$ [17, 18] along with the $SU(1, 1) \sim SO(2, 1)$ connection, we have constructed explicit form of $B_{n0}(p)$ (in a matrix representation of K^a [14] (see e.g. [16])). Computational details are in **Suppl. material A**. The free anyon solution is,

$$\begin{aligned} f_n^{a+} &= \left(\frac{2m}{E+m} \right)^\lambda \sqrt{\frac{\Gamma(2\lambda+n)}{n! \Gamma(2\lambda)}} \left(\frac{p^x + i p^y}{E+m} \right)^n \\ &\quad \times F^a(p) e^{-i p \cdot x} \end{aligned} \quad (7)$$

where $F^a(p)$ is same as the spin-1 case defined in (2). This is our primary result that we exploit to construct the wave packet and subsequent anyon beam.

(ii) **Conserved current for single anyon:** Next we derive the conserved probability current for anyon $\partial^\mu j_\mu^{(s=1-\lambda)} = 0$ where j_0^s is the probability density. Since the anyon model of [14] is an extension of the spin-1 case we can take a cue from the latter where the conservation law $\partial^\mu j_\mu^{(s=1)} = 0$ reads

$$\begin{aligned} \partial^\mu j_\mu^{(s=1)} &= \partial^0 [F^{0\dagger} F^0 + F^{x\dagger} F^x + F^{y\dagger} F^y] \\ &\quad - \partial^x [F^{0\dagger} F^x + F^{x\dagger} F^0] - \partial^y [F^{0\dagger} F^y + F^{y\dagger} F^0] = 0 \end{aligned} \quad (8)$$

Considering the Fourier transform of the anyon equation of motion (5) in position space, a long calculation yields the conserved free (single) anyon current $j_\mu^{(1-\lambda)}$,

$$\begin{aligned} \partial^0 \sum_{n=0}^{\infty} & \left[(f_n^{0\dagger} f_n^0 + f_n^{x\dagger} f_n^x + f_n^{y\dagger} f_n^y) - i(f_n^{y\dagger} K_{nn'}^0 f_n^x - f_n^{x\dagger} K_{nn'}^0 f_n^y) \right] \\ - \partial^x \sum_{n=0}^{\infty} & \left[(f_n^{0\dagger} f_n^x + f_n^{x\dagger} f_n^0) - i(f_n^{y\dagger} K_{nn'}^x f_n^x - f_n^{x\dagger} K_{nn'}^x f_n^y) \right] \\ - \partial^y \sum_{n=0}^{\infty} & \left[(f_n^{0\dagger} f_n^y + f_n^{y\dagger} f_n^0) - i(f_n^{y\dagger} K_{nn'}^y f_n^x - f_n^{x\dagger} K_{nn'}^y f_n^y) \right] = 0 \end{aligned} \quad (9)$$

where we have explicitly shown the summation over n , the anyonic index. For $\lambda = 0$ the current $j_\mu^{(1-\lambda)}$ reduces to the spin 1 current $j_\mu^{(1)}$ of (8). A nontrivial check of the consistency of the expressions for anyon current (9) is to substitute f_n^a from (7) to yield

$$\begin{aligned} j^0 &= (1-\lambda)E/m; \quad j^x = (1-\lambda)p^x/m; \\ j^y &= (1-\lambda)p^y/m \rightarrow j^\mu = (1-\lambda)\frac{p^\mu}{m} = s\frac{p^\mu}{m}. \end{aligned} \quad (10)$$

For computational details see **Suppl. material B**.

(iii) **Anyon wave packet:** Our aim is to construct the anyon current, not for a single anyon as done above, but for an anyon wave packet which can be amenable to experimental verification. Let us now construct the anyon wave packet that we want to move towards, say, $+x$ -direction. Since we have superposed plane waves, later figures will reveal that the current density has a sharply peaked profile with the y -component of current density having a comparatively reduced value. Note an important difference in geometry between our construction and that of the three-dimensional vortex beam [2]. In the latter case the free monoenergetic plane wave solutions (to be superposed) are distributed over the surface of a right circular cone with identical momentum amplitude in the propagation direction. However, for our anyon wave packet, in a planar geometry the above is not possible. Instead we use the superposition scheme where the azimuthal angle ϕ of momenta of the plane wave is integrated symmetrically from $\phi_0 = -\pi/2$ to $\phi_0 = +\pi/2$. In Fig. 1 we have shown profiles for charge density of anyon beam, J_0^λ , for $\lambda = 0.6 \rightarrow s = 1 - \lambda = 0.4$ for $\phi_0 = \pm\pi/2$.

Hence, considering superpositions of anyon plane waves with fixed spin $s = 1 - \lambda$, fixed energy E and fixed kinetic energy $p = \sqrt{(p^x)^2 + (p^y)^2}$, for the special case of integration limits $\phi_0 = \pm\pi/2$, the superposition F_n^a appears as

$$\begin{aligned} F_n^a(p, x) &= \mathcal{A}_n \int_{-\pi/2}^{\pi/2} \left[\left(1 + \frac{p^2}{M} \cos \alpha e^{i\alpha} \right) e^{i\alpha} \right. \\ &\quad \left. \left(i + \frac{p^2}{M} \sin \alpha e^{i\alpha} \right) e^{i\alpha} \right] \\ &\quad \left(e^{i(x \cos \alpha + y \sin \alpha)} + e^{i(x \cos \alpha - y \sin \alpha)} \right) d\alpha \end{aligned} \quad (11)$$

where $\mathcal{A}_n = \frac{1}{2} \left(\frac{2m}{E+m} \right)^\lambda \sqrt{\frac{\Gamma(2\lambda+n)}{n! \Gamma(2\lambda)}} \sqrt{\frac{m}{E}} \left(\frac{p}{E+m} \right)^n$, $x \equiv px$, $y \equiv py$ and $M = m(E+m)$. The expression is symmetric separately under $x \rightarrow -x$ and $y \rightarrow -y$.

Conserved current for anyon wave packet: The final analytical task is to substitute the anyon wave packet (11) in the expression of the anyon current (9). Since the current components are quadratic in the packet wavefunctions F_n^a , the final expressions are quite long and involved. We have shown only the expression for probability density J^0 and have relegated J^x and J^y to **Suppl. material C** together with a few computational steps. The cherished form of anyon beam probability density, in polar coordinates $x = \rho \cos \theta$, $y = \rho \sin \theta$, is

$$\begin{aligned} J^0(\rho, \theta) &= \left(\frac{2m}{E+m} \right)^{2\lambda} \frac{m}{E} \int_{-\pi/2}^{\pi/2} d\alpha \int_{-\pi/2}^{\pi/2} d\beta \left[e^{-2i\rho p \sin(\theta - (\alpha+\beta)/2) \sin((\alpha-\beta)/2)} + e^{-2i\rho p (\sin(\theta - (\alpha-\beta)/2) \sin((\alpha+\beta)/2)} \right. \\ &\quad \left. + e^{-2i\rho p (\sin(\theta + (\alpha-\beta)/2) \sin(-(\alpha+\beta)/2)} + e^{-2i\rho p (\sin(\theta + (\alpha+\beta)/2) \sin(-(\alpha-\beta)/2)} \right] \left[\left[1 - e^{-i(\alpha-\beta)} \sigma^2 \right]^{-2\lambda} \right. \\ &\quad \left. \left\{ \left(\frac{p}{2m} \right)^2 e^{-i(\alpha-\beta)} + \frac{1}{4} \left\{ (1+\lambda) \left(2 + \frac{2p^2}{M} \right) + \frac{p^4}{M^2} e^{-i(\alpha-\beta)} (\cos(\alpha-\beta) + i\lambda \sin(\alpha-\beta)) \right\} \right\} \right. \\ &\quad \left. - \frac{\lambda}{2} \left[\left[1 - e^{-i(\alpha-\beta)} \sigma^2 \right]^{-2\lambda-1} \left(2 + 2\frac{p^2}{M} + i\frac{p^4}{M^2} \sin(\alpha-\beta) e^{-i(\alpha-\beta)} \right) \right] \right] \end{aligned} \quad (12)$$

where, $\sigma = \left(\frac{p}{E+m} \right)$.

(iv) **Visualizing the anyon beam:** Unfortunately, closed form expressions for the anyon beam current components J^0 , J^x , and J^y are not possible to obtain. For different choices of λ and ϕ_0 the profiles of J^0 are given in **Suppl. material D**. Subsequently, in Fig. 2 and Fig. 3, for the above values of s , ϕ_0 , we have plotted the profiles of J^a , $a \equiv x, y$ respectively, in three ways: a two-dimensional plot of J^a against the polar angle θ for a few values of the (planar) radial distance ρ , panel (a) in each group of figures. Another two-dimensional graph of the same data as panel (a) with magnitude of J^a against θ for the same values of ρ is shown in panel (b). A density plot in co-ordinate plane x - y is given in panel (c). Finally, a three-dimensional plot of J^a in co-ordinate plane x - y is provided in panel (d). Note that in panel (a), each continuous curve represents a fixed polar distance in coordinate plane x - y with the height being a measure of J^a whereas in panel (b), the radial distance is a measure of the intensity of J^a . Hence the curves that are further away from the centre in panel (b) represent points that are closer to the coordinate plane x - y .

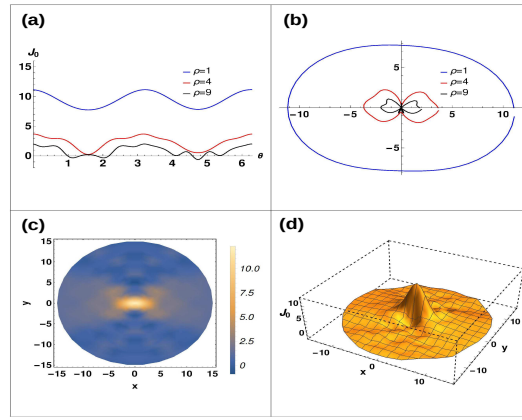


FIG. 1: (a) J^0 - θ for different values of ρ . (b) Polar plot for J^0 with θ for fixed ρ where the radial distance is the magnitude of J^0 . (c) Density plot of J^0 . (d) 3D plot of J^0 . We set $\lambda = 0.6$ and the integration range from $-\pi/2$ to $+\pi/2$.

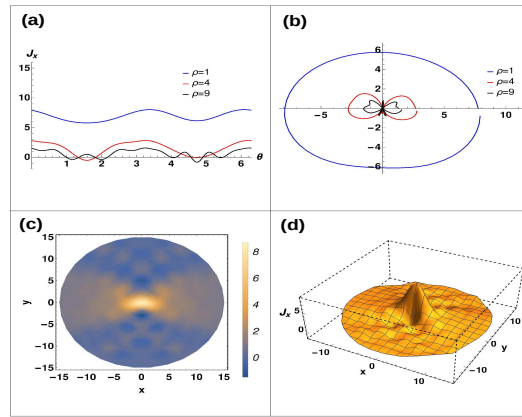


FIG. 2: J^x ($\lambda = 0.6$) with integration range $\pm\pi/2$, where (a)-(d) correspond to the similar meaning as described in Fig. 1.

As expected, all the wave packet profiles are symmetric about the abscissa since the packets are superposition of plane waves, that are symmetrically placed about the x -axis. Contrasting with the three-dimensional wave packets [2] it is clear that the planar anyon beams do not possess a vortex nature since the axial symmetry is manifestly broken while constructing a propagating anyon beam. This is also corroborated in the figures that do not have any destructive interference at the origin, a characteristic feature of vortex beams [2]. Hence the anyon beams are characterized by the spin value s of the wave packet, which is same as that of individual plane wave single anyon component.

An important observation is that in the cases we have considered, J^0 is always positive, which has to be the case since it is the probability density. But J^x is also positive throughout whereas J^y has positive and negative values

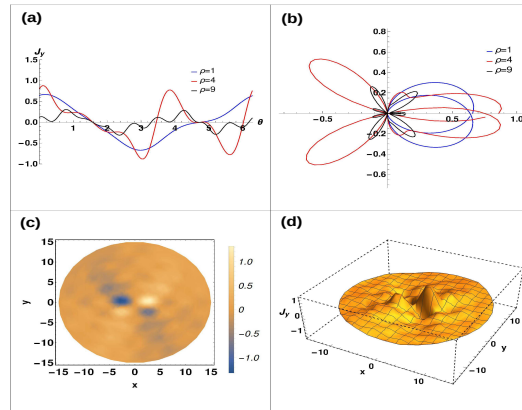


FIG. 3: J^y ($\lambda = 0.6$) with integration range $\pm\pi/2$, where (a)-(d) represent the similar meaning as described in Fig. 1.

in equal amount. Furthermore, maximum value of J^y is far lower than each of J^0 and J^x . These reflect the nature of our construction of the anyon beam where all the plane waves have *positive* velocity along x -direction but have pairwise *opposite* (both +ve and -ve) velocities along y -direction. Hence, the anyon beam will predominantly move in the positive x -direction with the y -component effectively canceled out.

(v) **Experimental possibilities:** Anyons were detected in quantum antidot experiments [19] and in Laughlin quasi-particle interferometer [20]. In relation to simulation of high T_c superconductivity by charged anyon fluid [21] their Josephson frequency has been observed [22] in 2D electrons in high magnetic field.

External electromagnetic field affects anyon with charge e and magnetic moment (see e.g. [2])

$$M = e \int dA (\epsilon_{ik} r^i j_s^k) / \int dA j_s^0 \quad (13)$$

for the single anyon current j_a^s (8) using (7). We replace j^a by J^a using the wave packet (11). The nonstationary quantum superposition state (wave packet) can be created by exciting matter coherently with an ultrafast laser pulse, which is composed of eigenstates spanned by the frequency bandwidth of the laser [23].

Possibility of fault tolerant quantum computation by (non-abelian) anyons has generated interest in controlled production of anyonic [13]: collective anyon excitations from electrons in the Fractional Quantum Hall (FQH) systems or from atoms in 1D optical lattices, creation of FQH effect for photons (using 1D or 2D cavity array), using a nonlinear

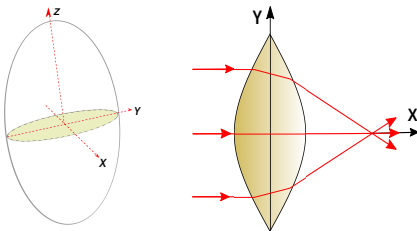


FIG. 4: Experimental setup: A slice (projection) of a 3D convex lens in the x - y plane (left diagram) is taken out and shown separately as thick lens in the right diagram. The red lines show the superposing wave vectors in x - y plane.

resonator lattice subject to dynamic modulation for creating anyons from photons, among others.

Topologically ordered many-body states (with quenched kinetic energy) are generated with strongly interacting particles in magnetic field. The system minimizes interaction energy forming intricate patterns of long-range entanglement as observed in FQH (semiconductor heterojunction, graphene [24, 25] and van der Waals bilayers [26]). Formation of Laughlin states in synthetic quantum systems (ultracold atoms [27, 28], photons [29–31]) have been developed. Recently in anyon optics, Laughlin states are made out of photon pairs (in a synthetic magnetic field for light induced from twisted optical cavity [32], strong photonic interactions via Rydberg atoms). These are modeled exploiting anyonic Hubbard Hamiltonian in ultracold-atom 1D lattices [33]. Anyon imaging with STM has also been achieved [33]. Theoretical [34, 35] and experimental [36] studies for simulating anyonic NOON states with photons in waveguide lattices have appeared.

Our experimental proposal: Following the work in [36], a two-photon NOON state with arbitrary anyonic symmetry is first prepared in a detuned directional coupler, and subsequently evolved in a Bloch oscillator emulated by a curved array. Then we use *planar analogue* of a spiral phase plate where phase shift proportional to the path length of the waves passing through the plate will occur. Upon superposition this will generate the anyon beam. This is schematically depicted in Fig. 4. The left panel of Fig. 4 shows a convex lens in three-dimensions x, y, z with parallel rays shown only along x - y plane that converge on x -axis. We consider an extremely thin slice of the lens in the x - y plane which can be thought as the shaded area in the left panel. The same slice is drawn separately in the right panel that shows the planar superposition in our work.

(vi) **Summary and future prospects:** We have suggested the construction of relativistic anyon beam, a symmetrical superposition of Jackiw-Nair single anyon solutions. Explicit forms of wave packets, their significant features and numerically plotted profiles of anyon beam current are given. A laboratory model of anyon beam construction is provided.

We thank Prof. V. Parameswaran Nair for actively helping us in this project.

[1] J. Durnin, J. Opt. Soc. Am. A **4**, 651 (1987);

[2] K. Y. Bliokh *et al.*, Phys. Rev. Lett. **99**, 190404 (2007); K. Y. Bliokh, M. R. Dennis, and F. Nori, Phys. Rev. Lett. **107**, 174802 (2011).

- [3] K. Y. Bliokh *et al.*, Phys. Rep. **690**, 1 (2017).
 [4] L. Allen *et al.*, Phys. Rev. A **45**, 8185 (1992).
 [5] A. J. Silenko, P. Zhang, and L. Zou, Phys. Rev. Lett. **121**, 043202 (2019).
 [6] F. Wilczek, Phys. Rev. Lett. **49**, 957 (1982).
 [7] J. M. Leinaas and J. Myrheim, Nuovo Cimento **37B**, 1 (1977).
 [8] *Fractional Statistics and Anyon Superconductivity*, World Scientific (1990), edited by F. Wilczek.
 [9] Y. Zhang *et al.*, Nature **438**, 201 (2005).
 [10] A. A. Zibrov *et al.*, Nature **549**, 360 (2017).
 [11] A. Yu. Kitaev, Ann. Phys. (N. Y.) **303**, 2 (2003).
 [12] H. Yao and S. A. Kivelson, Phys. Rev. Lett. **99**, 247203 (2007); M. Kapfer *et al.*, arXiv:1806.03117.
 [13] L. Savary and L. Balents, Rep. Prog. Phys. **80**, 016502 (2017); S. Dutta and E. J. Mueller, Phys. Rev. A **97**, 033825 (2018).
 [14] R. Jackiw and V. P. Nair, Phys. Rev. D **43**, 1933 (1991).
 [15] B. Binengar, J. Math Phys. **23**, 1511 (1982).
 [16] B. G. Wybourne, *Classical Groups for Physicists*, Wiley, New York (1974).
 [17] A. Perelomov, *Generalized coherent states and their applications*, Springer, Berlin (1986).
 [18] V. P. Nair, arXiv:1606.06407.
 [19] V. J. Goldman and B. Su, Science **267**, 1010 (1995); V. J. Goldman, J. Liu, and A. Zaslavsky, Phys. Rev. B **71**, 153303 (2005).
 [20] F. E. Camino, W. Zhou, and V. J. Goldman, arXiv:cond-mat/0611443.
 [21] Y. Hosotani, Int. J. Mod. Phys. B **7**, 2219 (1993); B. Abdullaev *et al.*, Phys. Rev. B **68**, 165105 (2003).
 [22] L. Yuan, M. Xiao, S. Xu, and S. Fan, Phys. Rev. A **96**, 043864 (2017).
 [23] L. J. Krause *et al.*, Phys. Rev. Lett. **79**, 4978 (1997).
 [24] X. Du *et al.*, Nature **462**, 192 (2009).
 [25] K. I. Bolotin *et al.*, Nature **462**, 196 (2009).
 [26] E. M. Spanton *et al.* Science **360**, 62 (2018).
 [27] I. Bloch, J. Dalibard, W. Zwerger, Rev. Mod. Phys. **80**, 885 (2008).
 [28] N. R. Cooper, J. Dalibard, I. B. Spielman, Rev. Mod. Phys. **91**, 015005 (2019).
 [29] R. Umucallar, M. Wouters, I. Carusotto, Phys. Rev. A **89**, 023803 (2014).
 [30] I. Carusotto, C. Ciuti, Rev. Mod. Phys. **85**, 299 (2013).
 [31] T. Ozawa *et al.* Rev. Mod. Phys. **91**, 015006 (2019).
 [32] C. Noh and D. G. Angelakis, Rep. Prog. Phys. **80**, 016401 (2017).
 [33] C. Yannouleas and U. Landman, Phys. Rev. A **100**, 013605 (2019).
 [34] Y. Bromberg, Y. Lahini, and Y. Silberberg, Phys. Rev. Lett. **105**, 263604 (2010).
 [35] S. Longhi and G. Della Valle, Opt. Lett. **37**, 2160 (2012).
 [36] M. Lebugle *et al.*, Nat. Commun. **6**, 8273 (2015).

Supplemental material for “Relativistic Anyon Beam: Construction and Properties”

Supplemental material A: Explicit form of the free anyon wavefunction

In order to compute the free anyon wavefunction from eq.(7) of main text we require explicit form of $B_{n0}(p)$ sector of the infinite component matrix $B_{nm'}(p)$. The best strategy is to use coherent states, given in Ref. [1], replacing z by a complex variable ω . The coherent states are obtained by quantization of the canonical one-form

$$dA = -i\lambda \left(\frac{\omega d\bar{\omega} - \bar{\omega} d\omega}{1 - \omega\bar{\omega}} \right). \quad (14)$$

These ideas have been discussed by Nair in [2]. This one-form defines a symplectic structure on $SU(1, 1)/U(1)$, where

$$g = \begin{pmatrix} 1 & \omega \\ \bar{\omega} & 1 \end{pmatrix} \frac{1}{\sqrt{1 - \omega\bar{\omega}}} \times \begin{pmatrix} e^{i\phi/2} & 0 \\ 0 & e^{-i\phi/2} \end{pmatrix} \quad (15)$$

The ϕ -part of g being irrelevant in dA , is not shown or equivalently we set $\phi = 0$. (Construction of normalized coherent states of $SU(1, 1)$ and its applications are discussed in [3].) The quantization of the canonical structure in (14) gives the coherent states given in [1] (in terms of $\omega, \bar{\omega}$ rather than z, z^*). One can view these coherent states as being given by the matrix element $g_{n0} \sim \langle \lambda, n | g | \lambda, 0 \rangle$. Here g_{nm} is the group element in the appropriate representation of g obeying the normalization condition $\sum_n g_{n0}^* g_{n0} = 1$. Let us now develop the Fock space $|\lambda, n\rangle$ in order to compute g_{n0} explicitly.

Our first task is to write g

$$g = \begin{pmatrix} 1 & \omega \\ \bar{\omega} & 1 \end{pmatrix} \frac{1}{\sqrt{1 - \omega\bar{\omega}}} \quad (16)$$

in a factorized form. The $SU(1, 1) \sim SO(2, 1)$ group generators and their commutation rules are given by

$$[K_0, K_{\pm}] = \pm K_{\pm}, \quad [K_+, K_-] = -2K_0 \quad (17)$$

where $K_{\pm} = K_1 \mp iK_2$. A matrix realization in terms of 2×2 Pauli matrices is

$$K_0 = \frac{1}{2}\sigma_3, \quad K_1 = \frac{i}{2}\sigma_1, \quad K_2 = -\frac{i}{2}\sigma_2. \quad (18)$$

Now it is straightforward to check that in the 2×2 matrix representation the following relation holds:

$$\begin{aligned} e^{-i\omega K_+} e^{\log(1-\bar{\omega}\omega)K_0} e^{-i\bar{\omega}K_-} &= \exp \left[\omega \begin{pmatrix} 0 & 1 \\ 0 & 0 \end{pmatrix} \right] e^{\sigma_3 \log(1-\bar{\omega}\omega)/2} \exp \left[\bar{\omega} \begin{pmatrix} 0 & 0 \\ 1 & 0 \end{pmatrix} \right] \\ &= \begin{pmatrix} 1 & \omega \\ 0 & 1 \end{pmatrix} \begin{pmatrix} \sqrt{1-\bar{\omega}\omega} & 0 \\ 0 & \frac{1}{\sqrt{1-\bar{\omega}\omega}} \end{pmatrix} \begin{pmatrix} 1 & 0 \\ \bar{\omega} & 1 \end{pmatrix} \\ &= g. \end{aligned} \quad (19)$$

Thus, we have managed to express g as a group element in a conventional form as the exponential of the generators with some parameters $\omega, \bar{\omega}$,

$$g = e^{-i\omega K_+} e^{\log(1-\bar{\omega}\omega)K_0} e^{-i\bar{\omega}K_-}. \quad (20)$$

This is precisely the infinite-dimensional bounded below representation of g [1] where the generators are to be taken in the representation of interest.

Returning to the Fock space construction, explicit form of the bounded below representation [1] is given by

$$\begin{aligned} K^0 | \lambda, n \rangle &= (\lambda + n) | \lambda, n \rangle; \\ K^+ | \lambda, n \rangle &= \sqrt{(2\lambda + n)(n + 1)} | \lambda, n + 1 \rangle; \\ K^- | \lambda, n \rangle &= \sqrt{(2\lambda + n - 1)n} | \lambda, n - 1 \rangle. \end{aligned} \quad (21)$$

The lowest state of the representation is defined by

$$K_- | \lambda, 0 \rangle = 0, \quad K_0 | \lambda, 0 \rangle = \lambda | \lambda, 0 \rangle \quad (22)$$

with higher states are obtained by the action of powers of K_+ on $|0\rangle$ in an obvious way, $K_0 K_+^m |0\rangle = (\lambda + m) K_+^m |0\rangle$. To recover the normalization we define $f(n)$ (see e.g. [4]),

$$\begin{aligned} f(n) &= \langle \lambda, 0 | K_-^n K_+^n | \lambda, 0 \rangle \\ &= \langle \lambda, 0 | K_-^{n-1} [K_-, K_+^n] | \lambda, 0 \rangle \\ &= \langle \lambda, 0 | K_-^{n-1} (2K_0 K_+^{n-1} + K_+ 2K_0 K_+^{n-2} + \dots + K_+^{n-1} 2K_0) | \lambda, 0 \rangle \\ &= 2 \sum_{k=1}^n (\lambda + n - k) f(n-1) \\ &= n(2\lambda + n - 1) f(n-1). \end{aligned} \quad (23)$$

Iterating and using $\langle 0 | 0 \rangle = 1$, we find $f(n)$ in a closed form:

$$f(n) = n!(2\lambda + n - 1)(2\lambda + n - 2) \dots (2\lambda) = \frac{\Gamma(n+1)\Gamma(2\lambda+n)}{\Gamma(2\lambda)} \quad (24)$$

where $\Gamma(u)$ is Eulerian gamma function for the argument u . The normalized states are thus given by

$$| \lambda, n \rangle = \frac{1}{\sqrt{f(n)}} K_+^n | \lambda, 0 \rangle \quad (25)$$

Finally the cherished form of matrix element g_{n0} in this representation is derived,

$$\begin{aligned} g_{n0} &= \langle \lambda, n | e^{-i\omega K_+} e^{\log(1-\bar{\omega}\omega)K_0} e^{-i\bar{\omega}K_-} | \lambda, 0 \rangle \\ &= \langle \lambda, n | e^{-i\omega K_+} e^{\log(1-\bar{\omega}\omega)\lambda} | \lambda, 0 \rangle \\ &= \langle \lambda, n | (-i\omega)^n \frac{K_+^n}{n!} | \lambda, 0 \rangle (1 - \bar{\omega}\omega)^\lambda \\ &= (-i\omega)^n (1 - \bar{\omega}\omega)^\lambda \sqrt{\frac{\Gamma(2\lambda+n)}{\Gamma(2\lambda)n!}} \end{aligned} \quad (26)$$

where we used $K_{\pm}^n | 0 \rangle = \sqrt{f(n)} | n \rangle$ from (12). A redefinition of variable ($-i\omega \rightarrow \omega$) yields,

$$g_{n0} = \sqrt{\frac{\Gamma(2\lambda + n)}{n!\Gamma(2\lambda)}} (1 - \bar{\omega}\omega)^{\lambda} \omega^n. \quad (27)$$

It is reassuring to check that the normalization condition mentioned earlier holds:

$$\begin{aligned} (g^{\dagger}g)_{00} &= \sum_n g_{n0}^* g_{n0} = \sum_n \frac{\Gamma(2\lambda + n)}{n!\Gamma(2\lambda)} (\bar{\omega}\omega)^n (1 - \bar{\omega}\omega)^{2\lambda} \\ &= \frac{(1 - \bar{\omega}\omega)^{2\lambda}}{\Gamma(2\lambda)} \sum_n \int_0^{\infty} dt e^{-t} \frac{t^{2\lambda+n-1} (\bar{\omega}\omega)^n}{n!} \\ &= \frac{(1 - \bar{\omega}\omega)^{2\lambda}}{\Gamma(2\lambda)} \int_0^{\infty} dt e^{-t} e^{t\bar{\omega}\omega} t^{2\lambda-1} \\ &= \frac{(1 - \bar{\omega}\omega)^{2\lambda}}{\Gamma(2\lambda)} \int_0^{\infty} dt e^{-t(1-\bar{\omega}\omega)} t^{2\lambda-1} \\ &= 1. \end{aligned} \quad (28)$$

The $SU(1,1) \rightarrow SO(2,1)$ map: The manifestly covariant field theoretic construction should reveal the single particle Poincare group representations of $SO(2,1)$ [5]. In the present scheme g , being an element of $SU(1,1)$ satisfies $\sigma_3 g^{\dagger} \sigma_3 = g^{-1}$, or equivalently $g^{\dagger} \sigma_3 g = \sigma_3$. The adjoint representation of this is defined by

$$R_{ij} = \frac{1}{2} Tr(g^{-1} K_{ig} K_j) \quad (29)$$

with R_{ij} being real since it obeys $K_i^{\dagger} \sigma_3 = \sigma_3 K_i$. Thus clearly R_{ij} is a real $SO(2,1)$ matrix. This is the $SU(1,1) \rightarrow SO(2,1)$ map.

To construct $B_{n0}(p)$, we start with Eq.(3.6) of [1],

$$B(p) = \frac{1}{\sqrt{2m}} [\sqrt{p \cdot \eta + m} + i \frac{1}{\sqrt{p \cdot \eta + m}} \epsilon^{abc} p_a \eta_b \gamma_c] \quad (30)$$

with the convention

$$\gamma^a = \{-\sigma^3, -i\sigma^2, i\sigma^1\}; \quad \gamma_a = \{-\sigma^3, i\sigma^2, -i\sigma^1\}; \quad \eta^a = \eta_a = \{1, 0, 0\}, \quad (31)$$

which gives B_{n0} in the 2×2 matrix representation.

We use this $B(p)$ in place of g in

$$B(p) \equiv g = \sqrt{\frac{E+m}{2m}} \begin{pmatrix} 1 & -\frac{p_-}{E+m} \\ -\frac{p_+}{E+m} & 1 \end{pmatrix} \quad (32)$$

where $p_{\pm} = p_x \pm ip_y$. The above is written as

$$B = \sqrt{\frac{1}{1-\omega\bar{\omega}}} \begin{pmatrix} 1 & \omega \\ \bar{\omega} & 1 \end{pmatrix} \quad (33)$$

where $\omega = \frac{p_-}{E+m}$, $\bar{\omega} = \frac{p_+}{E+m}$.

Substituting ω in (27)

$$g_{n0} = \sqrt{\frac{\Gamma(2\lambda + n)}{n!\Gamma(2\lambda)}} (1 - \omega\bar{\omega})^{\lambda} \omega^n = \sqrt{\frac{\Gamma(2\lambda + n)}{n!\Gamma(2\lambda)}} \left(\frac{2m}{E+m}\right)^{\lambda} \left(\frac{pe^{-i\phi}}{E+m}\right)^n \quad (34)$$

where $p_x = p \cos \phi$, $p_y = p \sin \phi$ and $p = \sqrt{p_x^2 + p_y^2}$.

The final expression is

$$g_{n0} = \sqrt{\frac{\Gamma(2\lambda + n)}{n!\Gamma(2\lambda)}} (2m)^{\lambda} (E+m)^{-(n+\lambda)} (pe^{-i\phi})^n = B_{n0}. \quad (35)$$

Supplemental material B: Computational Details

In deriving the anyon current we have used the matrix representations of K^a -matrices (see eq.(6) of main text) [1],

Let us define, $K_{nn'}^a = \langle \lambda, n | K^a | \lambda, n' \rangle$

Therefore, $K_{nn'}^0 = \langle \lambda, n | K^0 | \lambda, n' \rangle = (\lambda + n)\delta_{nn'}$, and

$K_{nn'}^+ = \langle \lambda, n | K^+ | \lambda, n' \rangle = \langle \lambda, n | (\sqrt{(2\lambda + n')(n' + 1)}) | \lambda, n' + 1 \rangle = \sqrt{(2\lambda + n - 1)n}\delta_{n, n'+1}$

similarly, $K_{nn'}^- = \langle \lambda, n | K^- | \lambda, n' \rangle = \sqrt{(2\lambda + n)(n + 1)}\delta_{n, n'-1}$

Now, $K^\pm = K^x \mp iK^y$

Therefore we finally have,

$$K_{nn'}^x = \frac{1}{2} (K_{nn'}^+ + K_{nn'}^-) = \frac{1}{2} \left(\sqrt{(2\lambda + n - 1)n}\delta_{n, n'+1} + \sqrt{(2\lambda + n)(n + 1)}\delta_{n, n'-1} \right)$$

$$K_{nn'}^y = \frac{i}{2} (K_{nn'}^+ - K_{nn'}^-) = \frac{i}{2} \left(\sqrt{(2\lambda + n - 1)n}\delta_{n, n'+1} - \sqrt{(2\lambda + n)(n + 1)}\delta_{n, n'-1} \right)$$

$$K_{nn'}^0 = (\lambda + n)\delta_{nn'} \quad (36)$$

and the identity

$$\sum_{n=0}^{\infty} \frac{\Gamma(a+n)s^n}{n!} = (1-s)^{(-a)}\Gamma(a); \quad |s| < 1. \quad (37)$$

Supplemental material C: Expression for anyon beam current

The spatial components of the anyon current built from the wavefunctions are:

$$\begin{aligned} J^x(\rho, \theta) = & \left(\frac{2m}{E+m} \right)^{2\lambda} \frac{m}{E} \int_{-\pi/2}^{\pi/2} d\alpha \int_{-\pi/2}^{\pi/2} d\beta \left[e^{-2i\rho p \sin(\theta - (\alpha + \beta)/2) \sin((\alpha - \beta)/2)} \right. \\ & + e^{-2i\rho p (\sin(\theta - (\alpha - \beta)/2) \sin((\alpha + \beta)/2)} + e^{-2i\rho p (\sin(\theta + (\alpha - \beta)/2) \sin(-(\alpha + \beta)/2)} \\ & \left. + e^{-2i\rho p (\sin(\theta + (\alpha - \beta)/2) \sin(-(\alpha + \beta)/2)} \right] \\ & \left[\frac{1}{2} \frac{p}{2m} \left\{ [1 - e^{-i(\alpha - \beta)} \sigma^2]^{-2\lambda} \left(e^{-i\frac{\alpha}{2}} + e^{i\frac{\beta}{2}} + \frac{2p^2}{M} e^{-i(\alpha - \beta)} \cos(\alpha + \beta/2) \cos(\alpha - \beta/2) \right) \right\} \right. \\ & \left. - \frac{i\sigma\lambda}{4} \left\{ [1 - e^{-i(\alpha - \beta)} \sigma^2]^{-2\lambda - 1} \left(e^{-i\frac{\alpha}{2}} + e^{i\frac{\beta}{2}} \right) \left(-2i - 2i\frac{p^2}{M} + \frac{p^4}{M^2} e^{-i(\alpha - \beta)} \sin(\alpha - \beta) \right) \right\} \right]. \quad (38) \end{aligned}$$

and

$$\begin{aligned} J^y(\rho, \theta) = & \left(\frac{2m}{E+m} \right)^{2\lambda} \frac{m}{E} \int_{-\pi/2}^{\pi/2} d\alpha \int_{-\pi/2}^{\pi/2} d\beta \left[e^{-2i\rho p \sin(\theta - (\alpha + \beta)/2) \sin((\alpha - \beta)/2)} \right. \\ & + e^{-2i\rho p (\sin(\theta - (\alpha - \beta)/2) \sin((\alpha + \beta)/2)} + e^{-2i\rho p (\sin(\theta + (\alpha - \beta)/2) \sin(-(\alpha + \beta)/2)} \\ & \left. + e^{-2i\rho p (\sin(\theta + (\alpha - \beta)/2) \sin(-(\alpha + \beta)/2)} \right] \\ & \left[\frac{1}{2} \frac{p}{2m} \left\{ [1 - e^{-i(\alpha - \beta)} \sigma^2]^{-2\lambda} \left(ie^{-i\frac{\alpha}{2}} - ie^{i\frac{\beta}{2}} + \frac{2p^2}{M} e^{-i(\alpha - \beta)} \cos(\alpha + \beta/2) \cos(\alpha - \beta/2) \right) \right\} \right. \\ & \left. + \frac{\sigma\lambda}{4} \left\{ [1 - e^{-i(\alpha - \beta)} \sigma^2]^{-2\lambda - 1} \left(e^{-i\frac{\alpha}{2}} - e^{i\frac{\beta}{2}} \right) \left(-2i - 2i\frac{p^2}{M} + \frac{p^4}{M^2} e^{-i(\alpha - \beta)} \sin(\alpha - \beta) \right) \right\} \right]. \quad (39) \end{aligned}$$

where, $\sigma = p/(E + m)$.

Below we provide a few computational steps leading to J^0 given in (12). J^0 is given by

$$J^0 = \sum_{n=0}^{\infty} [F_n^{0\dagger} F_n^0 + F_n^{x\dagger} F_n^x + F_n^{y\dagger} F_n^y - i(F_n^{y\dagger} K_{nn'}^0 F_n^x - F_n^{x\dagger} K_{nn'}^0 F_n^y)]. \quad (40)$$

Consider the first term in the RHS where we have used expressions for the wave packet given in (12)

$$\begin{aligned} \sum_{n=0}^{\infty} F_n^{0\dagger} F_n^0 &= \frac{1}{\Gamma(2\lambda)} \left(\frac{2m}{E+m} \right)^{2\lambda} \left(\frac{p}{2m} \right)^2 \left(\frac{m}{E} \right) \sum_{n=0}^{\infty} \frac{\Gamma(2\lambda+n)}{n!} \left(\frac{p}{E+m} \right)^{2n} \\ &\quad \int_{-\pi/2}^{\pi/2} \int_{-\pi/2}^{\pi/2} d\alpha d\beta e^{-in\alpha} e^{-i\alpha} \left[e^{-i(x \cos \alpha + y \sin \alpha)} + e^{-i(x \cos \alpha - y \sin \alpha)} \right] \\ &\quad e^{in\beta} e^{i\beta} \left[e^{i(x \cos \beta + y \sin \beta)} + e^{i(x \cos \beta - y \sin \beta)} \right]. \end{aligned} \quad (41)$$

Now we substitute $x = \rho p \cos(\theta)$ and $y = \rho p \sin(\theta)$ and after using some well known trigonometric identity and the relation $\sum_{n=0}^{\infty} \frac{\Gamma(2\lambda+n)}{n!} x^n = (1-x)^{-2\lambda} \Gamma(2\lambda)$, we finally arrive at

$$\begin{aligned} \sum_{n=0}^{\infty} F_n^{0\dagger} F_n^0 &= \left(\frac{2m}{E+m} \right)^{2\lambda} \frac{m}{E} \int_{-\pi/2}^{\pi/2} \int_{-\pi/2}^{\pi/2} d\alpha d\beta \\ &\quad \left[e^{-2i\rho p \sin(\theta - (\alpha + \beta)/2) \sin((\alpha - \beta)/2)} + e^{-2i\rho p \sin(\theta - (\alpha - \beta)/2) \sin((\alpha + \beta)/2)} \right. \\ &\quad \left. + e^{-2i\rho p \sin(\theta + (\alpha - \beta)/2) \sin(-(\alpha + \beta)/2)} + e^{-2i\rho p \sin(\theta + (\alpha - \beta)/2) \sin((-\alpha + \beta)/2)} \right] \\ &\quad \left[1 + e^{-i(\alpha - \beta)} \sigma^2 \right]^{-2\lambda} \left(\frac{p}{2m} \right)^2 e^{-i(\alpha - \beta)}. \end{aligned} \quad (42)$$

Now we write the expression for J^0 as below

$$J^0 = \sum_{n=0}^{\infty} \left[F_n^{0\dagger} F_n^0 + F_n^{x\dagger} F_n^x + F_n^{y\dagger} F_n^y + i\lambda (F_n^{y\dagger} F_n^x - F_n^{x\dagger} F_n^y) - i(2\lambda + n) (F_n^{y\dagger} F_n^x - F_n^{x\dagger} F_n^y) \right]. \quad (43)$$

so that we can use the properties of Gamma function easily. Similarly we can calculate $\sum_{n=0}^{\infty} F_n^{y\dagger} F_n^x$ as

$$\begin{aligned} \sum_{n=0}^{\infty} F_n^{y\dagger} F_n^x &= \left(\frac{2m}{E+m} \right)^{2\lambda} \frac{m}{E} \int_{-\pi/2}^{\pi/2} \int_{-\pi/2}^{\pi/2} d\alpha d\beta \\ &\quad \left[e^{-2i\rho p \sin(\theta - (\alpha + \beta)/2) \sin((\alpha - \beta)/2)} + e^{-2i\rho p \sin(\theta - (\alpha - \beta)/2) \sin((\alpha + \beta)/2)} \right. \\ &\quad \left. + e^{-2i\rho p \sin(\theta + (\alpha - \beta)/2) \sin(-(\alpha + \beta)/2)} + e^{-2i\rho p \sin(\theta + (\alpha - \beta)/2) \sin((-\alpha + \beta)/2)} \right] \\ &\quad \left[1 + e^{-i(\alpha - \beta)} \sigma^2 \right]^{-2\lambda} \frac{1}{4} \left(-i - \frac{ip^2}{M} \cos(\beta) e^{i\beta} + \frac{p^2}{M} \sin(\alpha) e^{-i\alpha} + \frac{p^4}{M^2} \sin(\alpha) \cos(\beta) e^{-i(\alpha - \beta)} \right). \end{aligned} \quad (44)$$

and similarly the other terms of J^0 can be calculated. Putting all the terms in Eq.(30) we find

$$\begin{aligned} J^0(\rho, \theta) &= \left(\frac{2m}{E+m} \right)^{2\lambda} \frac{m}{E} \int_{-\pi/2}^{\pi/2} d\alpha \int_{-\pi/2}^{\pi/2} d\beta \left[e^{-2i\rho p \sin(\theta - (\alpha + \beta)/2) \sin((\alpha - \beta)/2)} + e^{-2i\rho p \sin(\theta - (\alpha - \beta)/2) \sin((\alpha + \beta)/2)} \right. \\ &\quad \left. + e^{-2i\rho p \sin(\theta + (\alpha - \beta)/2) \sin(-(\alpha + \beta)/2)} + e^{-2i\rho p \sin(\theta + (\alpha - \beta)/2) \sin((-\alpha + \beta)/2)} \right] \left[1 - e^{-i(\alpha - \beta)} \sigma^2 \right]^{-2\lambda} \\ &\quad \left\{ \left(\frac{p}{2m} \right)^2 e^{-i(\alpha - \beta)} + \frac{1}{4} \left\{ (1 + \lambda)(2 + \frac{2p^2}{M}) + \frac{p^4}{M^2} e^{-i(\alpha - \beta)} (\cos(\alpha - \beta) + i\lambda \sin(\alpha - \beta)) \right\} \right\} \\ &\quad - \frac{\lambda}{2} \left\{ \left[1 - e^{-i(\alpha - \beta)} \sigma^2 \right]^{-2\lambda - 1} \left(2 + 2\frac{p^2}{M} + i\frac{p^4}{M^2} \sin(\alpha - \beta) e^{-i(\alpha - \beta)} \right) \right\}. \end{aligned} \quad (45)$$

Supplemental material D: A few more examples of J^0 profiles

In Fig. 5 we show the features of the anyon beam profile with numerical plots of J^0 for $\lambda = 0.2$ and superposition angle $\phi_0 = \pm\pi/2$. Again in Fig. 6 we have plotted J^0 for $\lambda = 0.6$ for superposition angles having limiting values of $\phi_0 = \pm\pi/3, \pi/6$. Description of the figures has already been given in the main text.

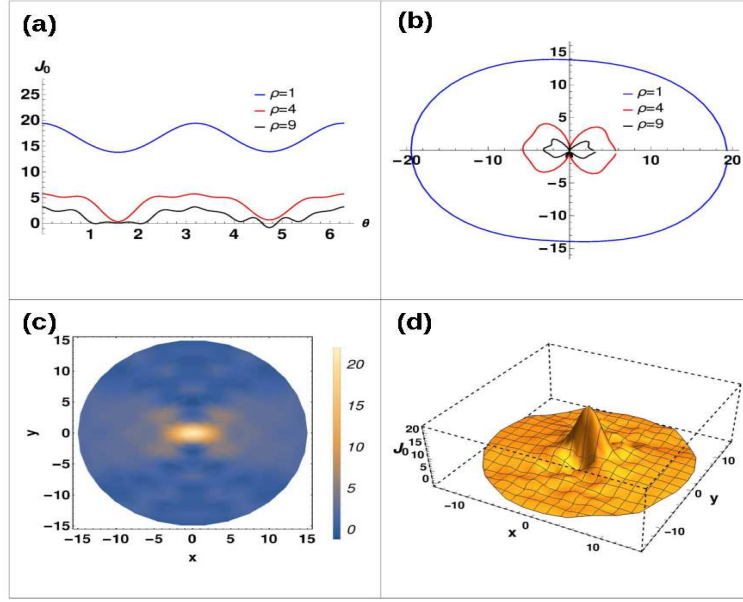


FIG. 5: (Color online). Same as Fig. 2 of the main article with $\lambda = 0.2$.

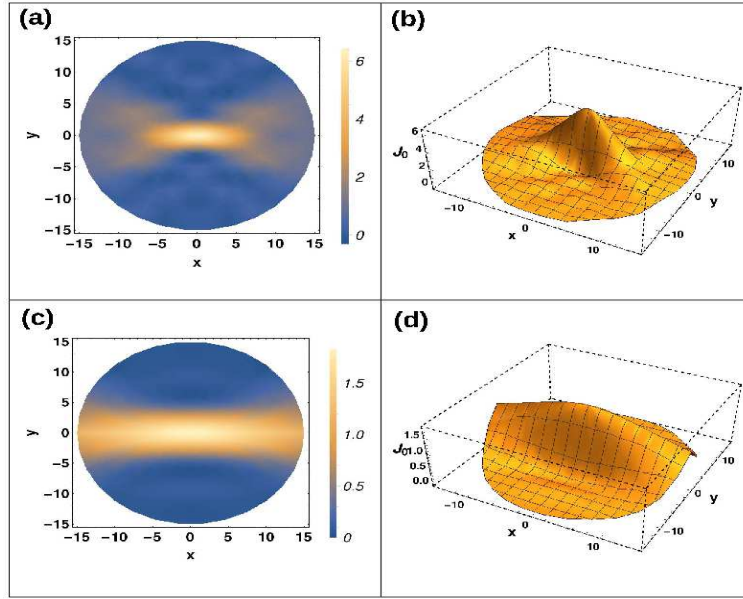


FIG. 6: (Color online). Density plot and the 3D plot of J^0 under two different integration ranges for superposition, considering $\lambda = 0.6$. In (a) and (b) we choose the integration range from $-\pi/3$ to $\pi/3$, while in (c) and (d) the range is taken from $-\pi/6$ to $\pi/6$.

We thank Professor V. Parameswaran Nair for actively helping us in this project.

-
- [1] R. Jackiw and V. P. Nair, Phys. Rev. D **43**, 1933 (1991).
 - [2] V. P. Nair, *Elements of Geometric Quantization and Applications to Fields and Fluids*, arXiv:1606.06407.
 - [3] A. Perelomov, *Generalized Coherent States and Their Applications*, Springer, Berlin (1986); for a short introduction see M. Novaes, Revista Brasileira de Ensino de Fisica **26**, 351 (2004).
 - [4] B. G. Wybourne, *Classical Groups for Physicists*, Wiley, New York (1974).
 - [5] B. Binengar, J. Math Phys. **23**, 1511 (1982).